Comparison of Simulated Orographic Precipitation Structures Using Different Microphysical Schemes With OLYMPEX Field Program Observations

Aaron R. Naeger[1] and Brian A. Colle[2]

[1]University of Alabama in Huntsville, Earth System Science Center/NASA SPoRT, Huntsville, AL [2]School of Marine and Atmospheric Science, Stony Brook University, Stony Brook, NY

aaron.naeger@nasa.gov

P108

Motivation and Goals

- Previous studies over the Pacific Northwest (e.g., IMPROVE-2; Garvert et al. 2005, Lin et al. 2009, etc.) showed many bulk micro schemes over-predict windward precipitation and snow aloft (too much cloud water lower over windward slope and too little near crest).
- There are large bulk microphysical parameter (BMP) uncertainties to riming and other ice characteristics (habit, size distribution, density, etc.).
- Orographic precipitation is also highly sensitive to the upstream cross barrier flow, moisture, and stability.
- There has been limited verification of orographic flooding events (high freezing levels) over Pacific Northwest (PNW).

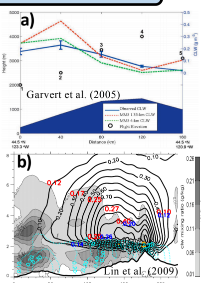

Figure 1. (a) Observed vs simulated cloud water, and (b) snow (red values and black contours) and cloud water (blue values and grey shades).

OLYMPEX Field Program

- Field observations included:

1. Coastal soundings; upstream flow, moisture, and stability
2. WSR-88D/NPOL; precip evolution around barrier
3. DOW/MRR; detailed precip structures over windward slope/valley
4. Gauges/Citation aircraft; spatial precip amounts and microphysics verification

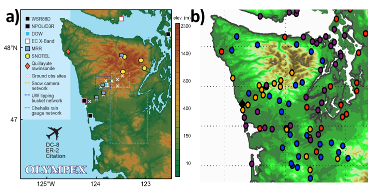

Figure 2. (a) OLYMPEX field observations. (b) All precip gauge sites.

Model Setup and Configuration

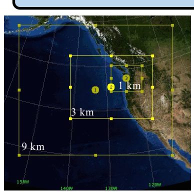

Figure 3. WRF model grid configuration

- Three heavy precip cases (12-13 Nov 2015, 17-18 Nov, 8-9 Dec) simulated using WRF model 3.7.1.
- IC/BCs: GFS, RUC, NARR, and GEFS
- MYJ PBL, Grell-Freitas (9 km), RRTMG
- 36-hour runs starting 12 Nov 12 UTC, 16 Nov 12 UTC, and 8 Dec 00 UTC. First 9-hour for spin-up.
- Implemented Predicted Particle Properties (P3) scheme (Morrison et al., 2015) into WRF model system.

BMP schemes

1. Thompson (THOMP); ~2D ice, ice size distribution from Field et al. (2005), variable riming efficiency.
2. Morrison (MORR); 2-moment, spherical ice/snow.
3. Stony Brook (SBU); ~2D ice/snow, combines snow/graupel into one category, degree of riming estimated and variations in snow density.
4. P3; Four prognostic mixing ratio variables predict the bulk particle properties of a single ice-phase. Advects ice/rime properties.

12-13 Nov 2015 Case Study

Synoptic-scale setup

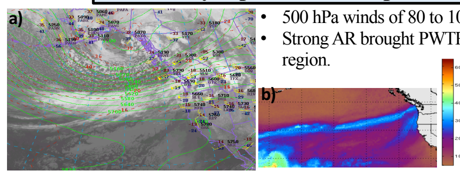

- 500 hPa winds of 80 to 100 knots over PNW.
- Strong AR brought PWTR of ~30 mm to the region.

Figure 4. (a) 500 hPa upper air observations and height contours overlaid on GOES IR image at 12 UTC 13 Nov, and (b) observed total precipitable water (PWTR) at 14 UTC.

Stability/Flow Evolution

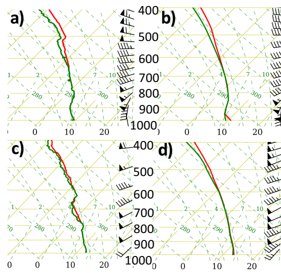

- Prior to 03 UTC 13 Nov – Stable layer between 950 and 800 hPa
- After 06 UTC 13 Nov – Near moist neutral
- Freezing level slowly rising from 2.3 to 2.7 km AMSL.
- WRF profiles show reasonable comparison to observations, but model is more stable at 09 UTC, especially between 800 and 700 hPa.

Figure 5. (a) Colorado State University (CSU) rawinsonde at NPOL site at 21 UTC 12 Nov, (b) WRF-P3 at same time. (c-d) Same as (a-b) but for 09 UTC Nov 13.

WSR-88D and station observations

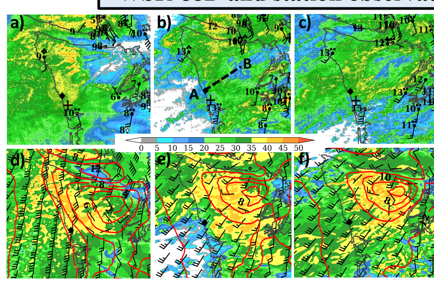

- WRF-P3 reflectivity shows overall good agreement with WSR-88D.
- However, model appears slightly fast by 12 UTC 13 Nov as obs show region of enhanced reflectivity further to the west off the coast.

Figure 6. Observed radar reflectivity at 0.5° elevation scan from WSR-88Ds at KRTX, KLGX, and KATX sites at (a) 21 UTC Nov 12, (b) 06 UTC Nov 13, and (c) 12 UTC Nov 13. Station observations are also shown at these times. (d-f) WRF-P3 reflectivity, 10-m winds, and 2-m temperatures from same times as in (a-c).

NPOL RHI cross sections

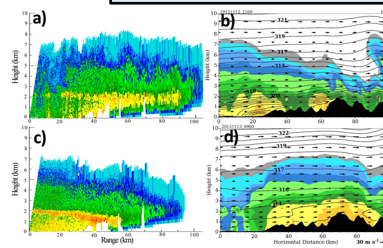

- Strong low-level stability in WRF-P3 at 21 UTC 12 Nov.
- Low-level stability diminishes by 09 UTC 13 Nov, which allows for heavier precip over terrain.
- NPOL obs also show this precip enhancement over terrain.

Figure 7. (a) Observed radar reflectivity along NPOL RHI scan at ~21 UTC 12 Nov, and (b) WRF-P3 reflectivity, equivalent potential temperature, and 3-dimensional wind circulation vectors for same time and cross section. (c-d) Same as (a-b), but for ~09 UTC 13 Nov.

WRF Hydrometeor cross sections

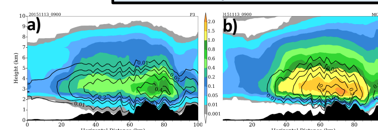

- MORR predicts much more snow aloft than P3.
- Rimed mass extends further to SW in cross section than graupel mass in MORR.

Figure 8. (a) WRF-P3 total ice (shaded) and rimed mass content (contoured) at 09 UTC 13 Nov. (b) Same as (a), but for WRF-MORR and graupel mass content. All units g m^{-3}.

UND citation and Precip Gauge sites

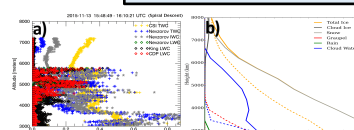

- MORR predicts too much snow aloft according to Citation measurements.
- Total ice from P3 shows much closer agreement to Citation.

Figure 9. (a) UND citation measurements of hydrometeor mass content during a spiral descent at ~1600 UTC 13 Nov. (b) Mass contents from WRF model output at 1430 UTC (MORR – solid, P3 – dashed).

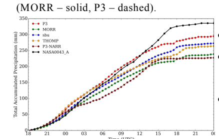

- All schemes underpredict precipitation for the event.
- Obs show heavy precip through 17 UTC while all model runs show minimal precip after 15 UTC.
- P3-NARR run is much drier than P3-GFS, which highlights the sensitivity to initial conditions.

Figure 10. Total accumulated precip from WRF model runs compared to NASA gauge site at Praire Creek.

Summary and Future Work

Large low-level stability early in the event resulted in flow splitting and maximum precip west of the lower windward slope, but as this stability decreased precip shifted over the higher terrain. WRF underpredicted precip over the lower windward slope by 10-30% with P3 simulating the most realistic amounts. MORR predicted too much snow aloft, and less riming and precipitation fallout over windward slope. Future work includes conducting additional simulations with updated P3 and Goddard 4ICE schemes, and further evaluating the schemes with an emphasis on the Goddard Satellite Data Simulator Unit (GSDSU).

*** This work is supported by grant NNX16AD81G.**